Detection of Broken Bars in the Cage Rotor on an Induction Machine

Nagwa M. Elkasabgy, Anthony R. Eastham, *Senior Member, IEEE,*
and Graham E. Dawson, *Senior Member, IEEE*

Abstract—**This paper describes techniques for the detection of broken bars in the cage rotor of an induction machine. A 30-hp four-pole induction machine with a deep-bar cage rotor was obtained from Canadian General Electric. Stator yoke, tooth tip and external search coils, and thermocouples were installed for test purposes. A shaft torque transducer was installed in line with a dc-load machine. The cross section of the machine was modeled with finite elements, and the field distribution and mechanical performance were computed using a nonlinear complex steady-state technique. Broken bars were shown to produce high localized airgap fields and to degrade mechanical performance. The field perturbation associated with broken bars, which are deliberately disconnected from the endrings by machining, produces low-frequency components and harmonics in the search coil-induced voltages and gives rise to an oscillatory torque that produces noise and mechanical vibration. Experimental results show that analysis of the voltage induced in an external search coil is adequate to detect the presence of broken bars.**

I. Introduction

IN RECENT years, the problems of failure in large machines have become more significant and of concern in industrial applications. The desire to improve the reliability of industrial drive systems has led to concerted research and development activities in several countries to evaluate the causes and consequences of various fault conditions. In particular, ongoing research work is being focused on rotor bar faults and on the development of diagnostic techniques [1]-[6].

Rotor failures are caused by a combination of various stresses that act on the rotor. In general terms, these stresses can be identified as electromagnetic, thermal, residual, dynamic, environmental and mechanical. If a motor is designed, built, installed, operated, and maintained properly, these stresses can be kept under control and the motor will function as intended for many years. However, inadequate casting or fabrication procedures, overloading, and lack of maintenance will lead to progressive deterioration of a drive. Detection techniques capable of identifying mechanical problems prior to failure are highly desirable, thereby allowing essential maintenance to be planned and avoiding costly and inconvenient downtime.

Paper IPCSD 91-77, approved by the Electrical Machines Committee of the IEEE Industry Applications Society for presentation at the 1988 Industry Applications Society Annual Meeting, Pittsburgh, PA, October 2-7. This work was supported by strategic and operating grants from the Natural Sciences and Engineering Research Council of Canada. Manuscript released for publication May 1, 1991.

The authors are with the Department of Electrical Engineering, Queen's University, Kingston, Ontario, Canada K7L 3N6.

IEEE Log Number 9103711.

Rotor fault conditions in induction motors have been examined primarily over the past decade by researchers such as Kliman [1], [2], Williamson [3], Deleroi [4], Gaydon [5], and others. These researchers have developed analyses and techniques to predict the change in motor performance as the rotor faults propagate. Attempts to develop instruments that would give an indication of broken bars while the motor is running on line have not yet been successful. These instruments depend on detecting a twice-slip frequency variation in the speed (or torque) [4], [5] or in the stator current frequency spectrum [1], [2]. The sensitivity of these techniques [1]-[5] is limited.

This paper uses field analysis to provide an accurate evaluation of the magnetic field distribution and mechanical performance of the machine. The complex stator and rotor lamination geometry, the spatial distribution of the conductors in the stator slots, and the effect of the nonlinearity of the magnetic material must be taken into account. The finite element technique is an effective numerical tool to solve the electromagnetic field equations [6] under these conditions.

This paper presents techniques for the detection of broken bars in a cage-rotor induction motor, which can be applied to motors operating under load. Some of the detection techniques depend on inserting search coils around a stator tooth tip or the stator yoke to detect the existence of the fault while others depend on access to the motor terminals. However, a simple, inexpensive, nonintrusive technique was found to be effective. This technique uses a search coil mounted on the motor frame and an analysis of the induced voltage waveform to detect the presence of broken bars.

II. Features and Assumptions of Method of Analysis

A 30-hp four-pole 460-V 60-Hz induction motor was obtained from Canadian General Electric and was used for both the analytical and experimental work. Analytically, a two-dimensional cross-section of the machine was modeled with 8736 finite elements and 4421 nodes to obtain a detailed representation of stator slot and bar conductor shapes. The discretization is shown in Fig. 1. In this paper, the nonlinear complex steady-state method for solving time varying problems in electric machines has been applied. The field variables, which are assumed to vary sinusoidally, are conveniently represented by phasors of the form $e^{j\omega t}$. Hence the partial differential operator $\partial/\partial t$ may be replaced by the arithmetic factor $j\omega$. The magnetic field is assumed to lie in the cross-sectional (x, y) plane, to be excited by and induce

0093-9994/92$03.00

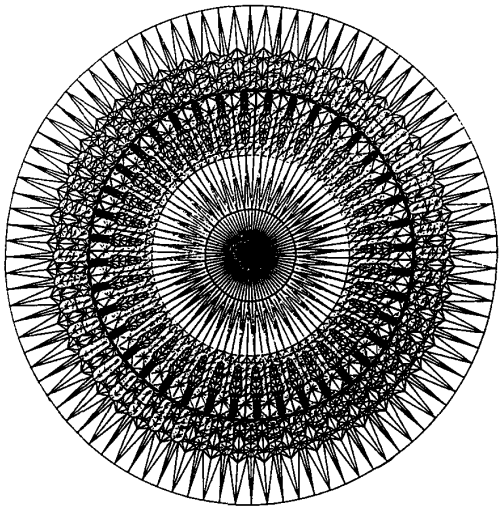

Fig. 1. Discretization of the 30-hp four-pole test machine.

only axial z-component currents, and to vary sinusoidally with time. The fundamental equation describing the space and time variation of the vector potential A over the region of analysis has the following form:

$$\partial/\partial x(1/\mu)\partial A/\partial x + \partial/\partial y(1/\mu)\partial A/\partial y - js\omega\sigma A + J = 0 \quad (1)$$

where s is the slip at a specific operating condition, μ is the permeability of the ferromagnetic material, σ is the conductivity of the conducting media in the rotor, and ω is the angular frequency.

If we assume that the three phase stator currents are

$$J_a = Je^{j\omega t}$$
$$J_b = Je^{j(\omega t + 2\pi/3)}$$
$$J_c = Je^{j(\omega t - 4\pi/3)} \quad (2)$$

then the magnetic vector potential at each nodal point in the machine discretization (Fig. 1) is similarly a sinusoidal function of time:

$$A(x, y) = Ae^{j(\omega t - \phi)} \quad (3)$$

where ϕ is the phase angle of the local magnetic vector potential.

The boundary conditions that are necessary to solve (1) are the following:

1) A is constant along the outside circumferential boundary. This implies that no field lines cross this boundary, i.e., that all flux paths close within the structure of the machine.
2) There is a periodicity condition along radial boundaries enclosing one pole pitch of the machine. When the entire cross-section of the machine must be analyzed (when no symmetry conditions exist, as for broken bars) only the boundary condition in (1) is applied.
3) When the flux leakage needs to be calculated, more layers of discretisation are added on the outer surface of the stator and the boundary conditions (1) is assigned to the outer surface of the last layer.

The conductivity of ferromagnetic regions is zero, and the permeability is μ_0 in nonmagnetic regions. In the stator and rotor cores, permeability is determined by the absolute value of the flux density, with reference to a magnetization curve stored as a look-up table (LUT) (with cubic spline interpolation between discrete points). The permeability is calculated at each step of numerical iteration from the previously calculated flux density B [7].

To model one or more broken bars, the bar current is set to zero by assigning zero conductivity to specific bar cross-sections. The analysis described in this paper is quite general as there is no restriction on the distribution of the broken bars.

Typical field distributions for a motor with no rotor faults and for one with five broken bars are shown in Fig. 2. The field distribution has been calculated at full load, i.e., at a speed of 1760 r/min. The broken bars lead to an enhanced field around the fault because of the lack of local demagnetizing slip frequency induced current in these rotor slots.

Fig. 3 shows flux density distributions in the airgap of the motor for various fault conditions, i.e., one, three, and five broken bars. For the fault-free rotor, the four-pole field distribution is symmetric, with superimposed slot ripple. For one, three, and five broken bars, the flux density becomes progressively higher in magnitude close to the fault, as is evident from the field distribution shown in Fig. 2.

The locally perturbed field distribution results in a degradation in the mechanical performance of the motor and causes torque harmonics. The results of finite element analysis were also used to calculate the torque–slip frequency characteristics of the motor. The effect of the various fault conditions is shown in Fig. 4. The results show that, in case of one broken bar, the degradation in the steady-state torque performance is in the order of 2–4%, whereas for three and five broken bars it is between 10–15%, for a motor with 40 rotor bars.

III. Experimental Detection Program

For experimental purposes, components of a four-pole 30-hp induction motor were obtained from Canadian General Electric and assembled with stator search coils and thermocouples to allow yoke, tooth tip and external flux densities, and winding temperatures to be monitored at various locations around the stator. The motor was mounted on a test bed and connected through a shaft speed/torque transducer to a dc-load machine. The test motor was excited with a 0–600 V 60-Hz 200-kVA three-phase variac. In one rotor, bars were deliberately separated from the endrings by careful machining. Different detection techniques show that the fault is readily detectable by low-frequency components of search coil induced voltage as well as by components in voltage and current waveforms separated from the fundamental by twice the slip frequency of the running condition. These frequency components can be observed in the time domain by means of an oscilloscope, or in the frequency domain by means of a

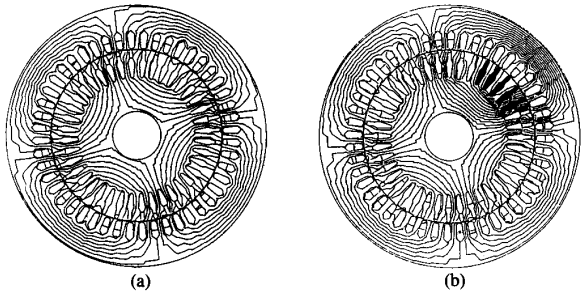

Fig. 2. Field distribution at full load (1760 r/min): (a) No broken bars; (b) five broken bars (shown shaded).

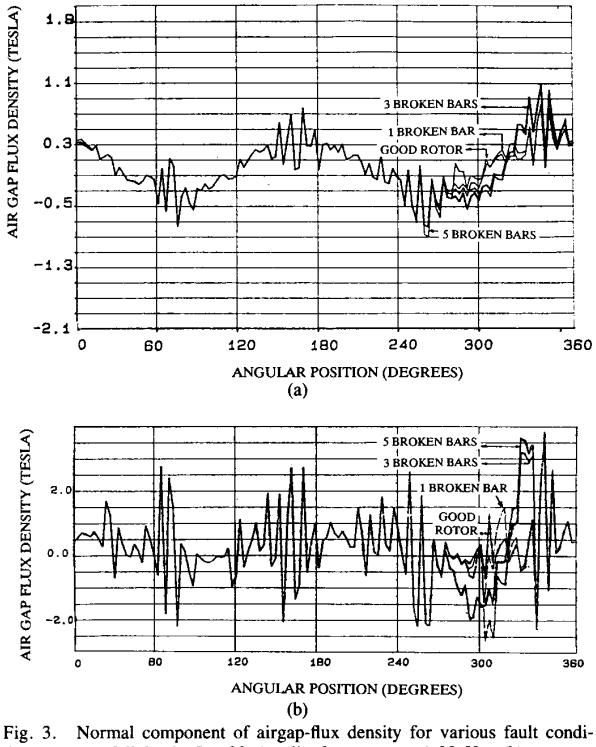

Fig. 3. Normal component of airgap-flux density for various fault conditions. (a) At full load; I = 38 A, slip frequency = 1.33 Hz; (b) at start; I = 196 A, slip frequency = 60 Hz.

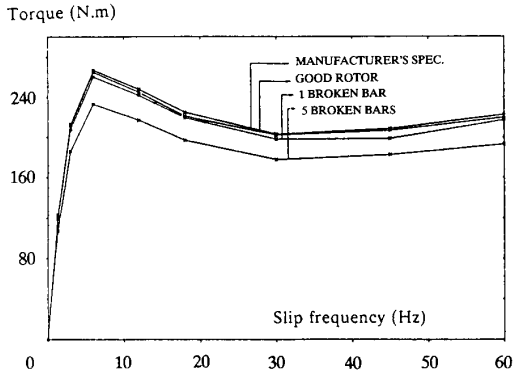

Fig. 4. Computed torque-slip frequency characteristics for the 30-hp induction motor with zero, one, and five broken bars.

spectrum analyzer. In addition, a fast IBM-PC-based data acquisition system was used to acquire test data from the motor and to store it on disk for processing and plotting.

In this paper, four different experimental techniques are presented and compared for the detection of broken bars: the induced voltages in search coils located both internally and externally, stator current harmonics, and torque harmonics. In the following sections, each technique is discussed.

A. Search Coil Induced Voltage Detection Techniques

This technique involves the inspection of a search coil induced voltage either as a time function or in the frequency domain. Consider first the voltage induced in an internal stator tooth tip coil for a machine with no rotor faults. The dominant and fundamental frequency will be at the motor excitation frequency of 60 Hz. Higher frequency components will appear due to the periodicity of rotor bars. The nonsinusoidal stator mmf distribution, i.e., space harmonics, may also induce time-harmonic voltages.

Consider now the voltage in the same search coil for a machine with one or more adjacent broken bars. Fig. 2 has shown that an anomalously high airgap local field rotates at rotor speed. This field pulsates at slip frequency and can be considered to be the resultant of two fields, counterrotating at s x synchronous speed, which are rapidly attenuated away from the fault location. The field associated with the broken bars will, therefore, modulate the coil-induced voltage at a characteristic frequency f_{fault}, given by

$$f_{fault} = \left(\frac{2f}{p}\right)(1 - s) \pm sf \text{ Hz} \tag{4}$$

where f is the excitation frequency, s is the slip, and p is the number of poles of the induction motor.

Similar frequency components are anticipated in the yoke and external search coil voltages. These voltages were captured by the fast data acquisition system and printed out to illustrate their time dependence. Their frequency spectra was also analyzed.

Numerous tests were observed for different operating conditions, i.e., no load at 1799 r/min, quarter load at 1790 r/min, half load at 1780 r/min, and full load at 1760 r/min. The tests were also run at different levels of applied voltage to examine the effect of saturation on the results.

Typical results are shown in Fig. 5, in which the stator tooth tip-coil voltages are compared for machines with no rotor fault and with five broken bars at full load (1760 r/min). Similar results for the yoke-coil voltages are also compared for the fault-free and the broken bar rotor at full load in Fig. 6. In Fig. 7, the external coil voltage is shown at the same operating condition. According to (4), the dominant fault frequencies should be 28.0 and 30.7 Hz (at 1760 r/min). This low-frequency modulation of all search-coil voltages is clearly evident. Observations of these voltages on an oscilloscope shows that the low-frequency fault signal "moves through" the fundamental voltage at a "speed" dependent on slip, as expected from (4).

The frequency spectra of these waveforms is also shown in Figs. 5–7. Comparing the tooth-tip search coil induced volt-

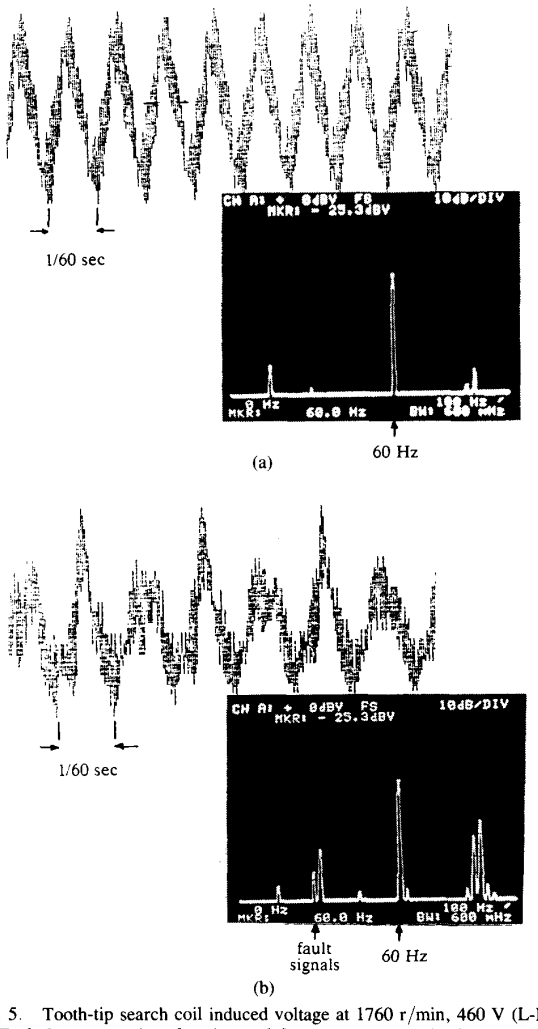

Fig. 5. Tooth-tip search coil induced voltage at 1760 r/min, 460 V (L-L): (a) Fault-free rotor (time function and frequency spectrum); (b) rotor with five broken bars (time function and frequency spectrum).

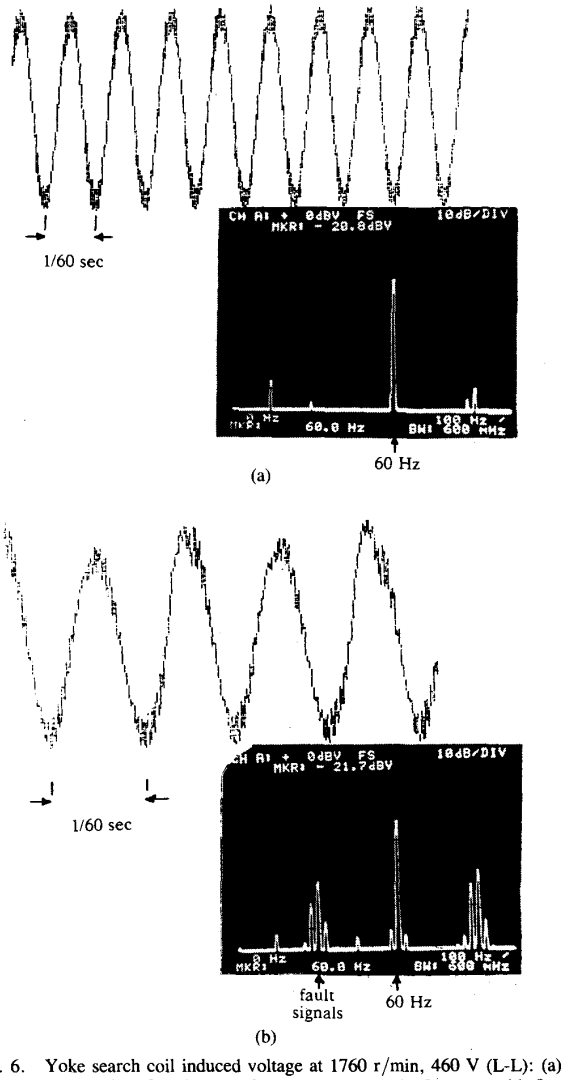

Fig. 6. Yoke search coil induced voltage at 1760 r/min, 460 V (L-L): (a) Fault-free rotor (time function and frequency spectrum); (b) rotor with five broken bars (time function and frequency spectrum).

age frequency spectrum for a fault-free rotor with that for the broken-bar rotor, the magnitude of the 28-Hz fault frequency component is −53 db and −30 db, respectively, relative to the 60-Hz component.

The same comparison was repeated for the yoke-search coil, where the 28-Hz frequency component for the broken-bar rotor is the dominant fault signal, with a magnitude of −28 db relative to the 60-Hz component. The external coil voltage also shows the 28-Hz frequency component for the broken-bar rotor, at −10 db relative to the fundamental as compared with −30 db for the fault-free rotor.

The appearance of fault frequency components in induced search-coil voltages is clearly an effective method of detecting broken bars. Although not presented here, the test results showed that the fault frequency components become more significant as the load is increased and as the stator voltage is increased. Perhaps surprisingly, the external search coil is just as effective as the internal coils in detecting the broken bars. It therefore appears unnecessary to incorporate internal coils to take advantage of this diagnostic technique; an external coil placed against the casing of the machine being entirely adequate.

B. Stator-Current Detection Technique

Based on the analyses presented in [3], [4], each individual rotor bar can be considered to form a short-pitched single-turn single-phase winding. The airgap field produced by a slip-frequency current flowing in a rotor bar will have a fundamental component rotating at slip speed in the forward direction with respect to the rotor, and one of equal amplitude that rotates at the same speed in the backward direction. With a symmetrical rotor, the backward components will sum to zero. For a broken-bar rotor, however, the resultant is nonzero. The field, which rotates at slip frequency backward with respect to the rotor, will induce EMF's in the

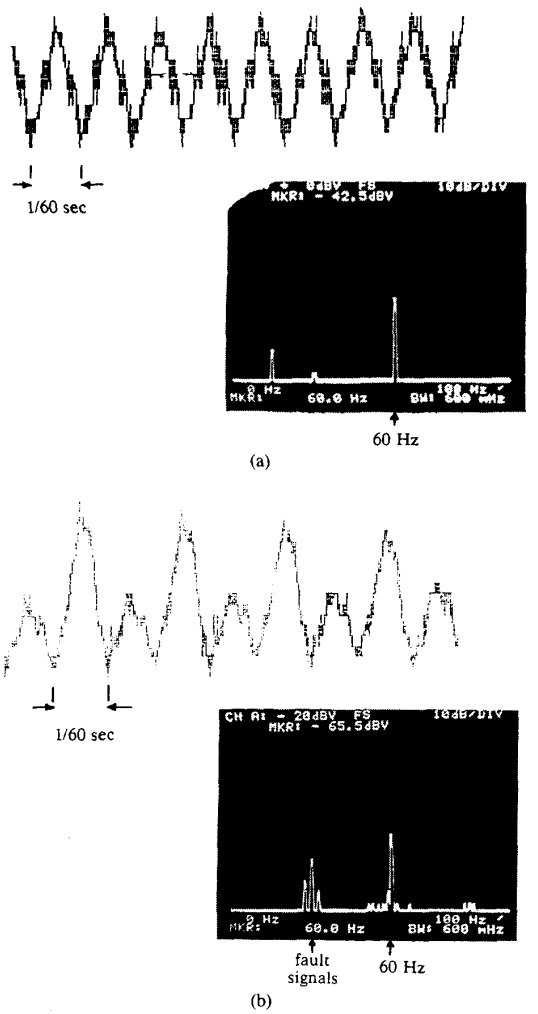

Fig. 7. External search coil induced voltage at 1760 r/min, 460 V (L-L): (a) Fault-free rotor (time function and frequency spectrum); (b) rotor with five broken bars (time function and frequency spectrum).

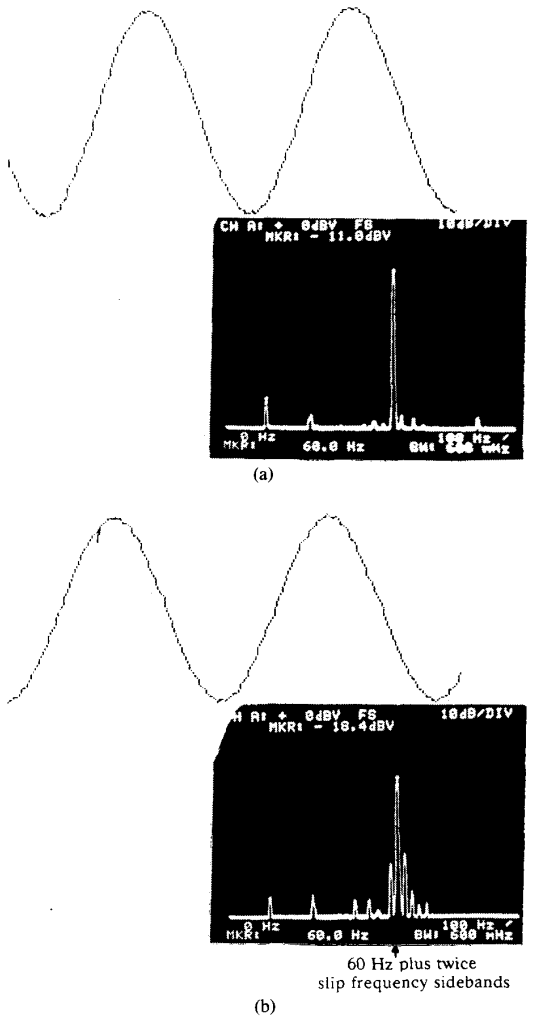

Fig. 8. Stator current at 1760 r/min, 460 V (L-L): (a) Fault-free rotor (time function and frequency spectrum); (b) rotor with five broken bars (time function and frequency spectrum).

stator side that modulate the mains-frequency component at twice slip frequency.

Under sinusoidal voltage excitation, this effect produces twice-slip frequency (2.67 Hz at 1760 r/min) side bands in the spectrum of the phase current. In Fig. 8, typical results are given for the stator current at full-load condition (1760 r/min), where the fundamental side bands at twice-slip frequency, 2.67 Hz indicate the existence of the fault. In the same figure the current spectrum for a fault-free rotor running at the same operating condition does not show the twice-slip frequency side bands. As found by other authors [3], [4], an examination of the machine current spectrum provides a second method for detecting rotor-bar faults.

C. Torque-Harmonics Detection Technique

In a balanced three-phase induction machine with no rotor faults, the forward-rotating field interacts with the slip frequency induced rotor currents to produce a steady output torque. For a machine with a rotor fault, a backward rotating field is developed as discussed. This backward rotating field interacts with the rotor currents, induced by the forward rotating field, to produce a torque variation at twice-slip frequency, which is superimposed on the steady output torque.

Rotor faults therefore lead to low-frequency torque harmonics, which result in increased noise and vibration. The torque oscillations were measured by means of a shaft torque transducer using the data acquisition system while the motor was running on-line at various load conditions. Fig. 9 shows typical experimental torque results for a rotor with five broken bars compared to a fault-free rotor. The frequency of the torque oscillation increases as the machine is loaded. In all the three cases, the dominant frequency of oscillation corresponds to twice the slip frequency of the operating condition.

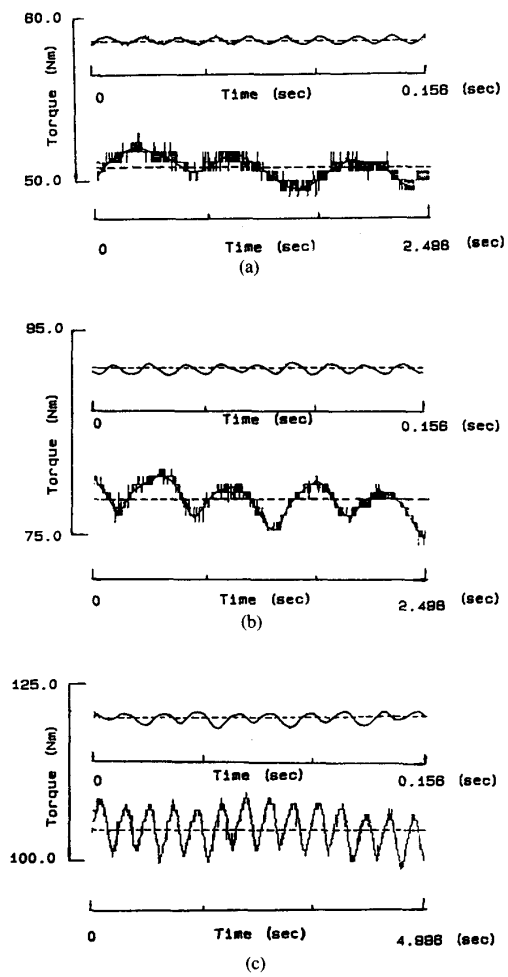

Fig. 9. Torque oscillation for the fault-free rotor (upper) and for the rotor with five broken bars (lower) at speeds of (a) 1780, (b) 1770, and (c) 1760 r/min.

IV. Summary of Detection Techniques

The finite element analysis has been used to examine the effects of broken bars in induction machines. The analysis clearly shows the effect of the fault on motor performance (electromagnetic and mechanical). The fault degrades the steady-state torque-slip frequency characteristic progressively as the number of broken bars increases. Four different techniques for the detection of broken bars were tested and evaluated:

1) An inspection of the time and frequency domain of voltages induced in internal (stator tooth tip and yoke) search coils
2) an inspection of the time and frequency domain of voltages induced in an external search coil placed against the frame of the motor
3) an inspection of the frequency domain of the stator current waveform
4) an inspection of the harmonic content of the shaft torque.

All methods were sensitive to the effects of a rotor fault, which were expected from consideration of the time-varying electromagnetic field distribution in the machine.

The first two methods involving search coil voltages appeared to provide the most useful, reliable, and cost-effective diagnostic techniques. It is concluded that broken bars may be adequately detected by examining the time domain or the frequency spectrum of search-coil voltages. The use of an external coil placed against the frame of the machine is considered particularly useful in an industrial environment because the motor need not be modified in any way (by prior installation of stator search coils) or be taken out of service temporarily. All that is needed is a coil of 10–20 turns of length equivalent to the active axial length of the machine and of width equal to perhaps half a pole, a power-frequency oscilloscope or low-frequency spectrum analyzer, and the eye of an observant operator.

References

[1] G. B. Kliman, "The detection of faulted rotor bars in operating induction motors," in *Proc. Int. Conf. Electric Machines* (ICEM86) (Munich, Germany), Sept. 1986, pp. 500–502.
[2] G. B. Kliman, R. A. Koegl, J. Stein, R. D. Endicott, and M. W. Madden, "Noninvasive detection of broken bars in operating induction motors," *IEEE Trans. Energy Conv.*, vol. 3, no. 4, pp. 873–874, 1989.
[3] S. Williamson and A. C. Smith, "Steady state analysis of 3-phase cage motors with rotor-bar and end-ring faults," in *Proc. Inst. Elec. Eng.*, vol. 129, no. 3, pp. 93–100, 1982.
[4] W. Deleroi, "Der stabbruch im kaufiglaufer eines asychonomotor," *Archiv für Elektrotechnik*, vol. 67, pp. 91–99, 1984.
[5] C. Hargis, B. G. Gaydon, and K. Kamash, "The detection of rotor defects in induction motors," in *Proc. Int. Conf. Electrical Machines—Design Applications* (London), July 1982, pp. 216–220.
[6] N. M. Elkasabgy, A. R. Eastham, and G. E. Dawson, "The detection and effects of broken bars in cage rotor induction machines," in *Proc. IEEE Workshop Electromagn. Field Comput.* (Schenectady, NY), Oct. 1986, pp. G24-G28.
[7] D. A. Lowther and P. P. Silvester, *Computer-Aided Design in Magnetics*. New York: Springer-Verlag, 1986.

Nagwa M. Elkasabgy received the B.Sc degree from Ain Shams University in 1976 and the M.Sc. degree from McMaster University in 1978 for work in power systems.

After periods of research at the Federal University of Rio de Janeiro and at the Military Institute of Engineering JME/RJ, she undertook doctoral studies at Queen's University. She received the Ph.D. degree for work on the detection of rotor faults in induction machines in 1988. After an appointment at Ryerson Polytechnical Institute in

Toronto, she returned to Queen's University to work in the area of robotics systems.

Anthony R. Eastham (M'75–SM'83) received the B.Sc degree in physics from the University of London and the Ph.D. degree from the University of Surrey, England, in 1965 and 1969, both in physics.

After research positions at Plessey Telecommunications Ltd. and at the University of Warwick, he moved to Canada in 1972, where he joined the Canadian Institute of Guided Ground Transport. He is now a professor of electrical engineering at Queen's University in Kingston, Ontario, having joined the faculty in 1978. His research activities include innovative urban and high-speed transportation, linear and rotary electrical drives, and electromagnetic analysis. Administratively, he serves as Director of Research Services and of International Programs at Queen's University.

Dr. Eastham is a Registered Professional Engineer of the Province of Ontario, Director of IEEE Canada, and past-president of the High Speed Rail Association.

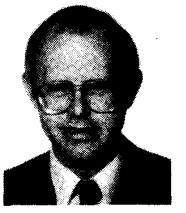

Graham E. Dawson (S'66–M'69–SM'91) received the B.A.Sc., M.S., and Ph.D. degrees from the University of British Columbia in 1963, 1966, and 1970, respectively.

In 1969, he joined the Department of Electrical Engineering at Queen's University at Kingston as an Assistant Professor. He was promoted to Associate Professor in 1975 and Professor in 1981. His electrical engineering research activities have been associated with the transportation industry, and his current interests are in computer-aided design and performance of rotary and linear traction motors and energy management of transportation systems.

Dr. Dawson is a Registered Professional Engineer in the Province of Ontario.